

## Design and Construction of a Miniature PIV (MPIV) System

Olivier Chetelat\*, Sang Youl Yoon, Kyung Chun Kim

School of Mechanical Engineering, Pusan National University, Busan 609-735, Korea

For two decades, there has been an active research to enhance the performances of Particle Image Velocimetry (PIV) systems. However, the resulting systems are somewhat very costly, cumbersome and delicate. In this paper, we address the design and some first experimental results of a PIV system belonging to the opposite paradigm. The *Miniature* PIV or MPIV system features relatively modest performances, but is considerably smaller (our MPIV could hold in dia. 40 mm×120 mm), cheaper (our MPIV total cost is less than \$ 500) and easy to handle. Potential applications include industrial velocity sensors. The proposed MPIV system uses a one-chip-only CMOS camera with digital output. Only two other chips are needed, one for a buffer memory and one for an interfacing logic that controls the system. Images are transferred to a personal computer (PC or laptop) via its standard parallel port. No extra hardware is required (in particular, no frame grabber board is needed). In our first MPIV prototype presented in this paper, the strobe lighting is generated by a cheap 5 mW laser pointer diode. Experimental results are presented and discussed.

**Key Words :** Miniature Image Particle Velocimetry (MPIV), CMOS Camera, Laser Pointer

### 1. Introduction

*Particle Image Velocimetry* (PIV) is a technique for measuring the velocity field of gas or liquids. The field is usually limited to a planar subspace and the velocity is described by vectors lying in this plane. However, 3D PIVs are also possible.

The idea of PIV is to observe particles carried by the flow to measure. The particles should be small enough to faithfully follow the flow velocity variations, but big enough to be seen by a camera. Indeed, a strobe light (or sometimes the camera shutter) is used to take snapshots of the particle positions at different instants. Image processing techniques can then compute the velocity field (and possibly other fields, like rotational, di-

vergence, acceleration, etc.). The flow may naturally contain particles, such as dust, pollen, bubbles, plankton, etc, or may be artificially seeded, e. g. with oil droplets or hollow glass balls. An overview of modern PIV as well as other similar non-invasive optical techniques for flow velocity measurements can be found in Degrez and Riethmuller (1994), Lourenco (1996) and Stanislas and Monnier (1997).

So far, the PIV technique has been mainly developed to study flows. The commercially available systems tend to be more and more enhanced rather than cheaper and easier to use, even though they are intrinsically both cheaper and easier to use if compared with the same features offered by earlier systems. Most of PIV systems usually are still designed for flow engineers and researchers who used them as measurement instruments to help them in their design optimization or in their physics understanding. PIV systems used as industrial sensors could however be of interest even if their performances as PIV measurement instrument are

\* Corresponding Author,

E-mail : chetelat@pusan.ac.kr

TEL : +82-51-510-2490; FAX : +82-51-582-8581

School of Mechanical Engineering, Pusan National University, Busan 609-735, Korea. (Manuscript Received July 31, 2001; Revised September 15, 2001)

not at the best of the current art. Our concept of MPIV (miniature PIV) systems aims to reduce not only the cost and the size, but also the amount of time and expertise needed for setup and maintenance.

For PIV as sensors, natural particles are of first interest since the velocity can be measured without the need of a seeding device. A seeding extra device may indeed unacceptably increase the maintenance load since particles are consumables. As the MPIV system includes a camera with an illumination system, it can also provide relevant information about the density, size or nature of natural particles in addition to flow velocity vectors. In some applications, such as paint spray, the particles themselves rather than the flow may be the measurement object. A good control and monitoring of paint spray is important since the quality of painting is directly related to the velocity and size of the paint droplets.

This paper mainly presents the MPIV hardware and architecture. The described illumination is realized using a 5mW laser diode in a classical PIV configuration (the laser beam is shaped into a light sheet that defines the measurement plane), but other (possibly better) options are possible. In Chetelat et al. (2001), other illumination options are presented, in particular a backward illumination (the light comes from behind the particles) realized with a dozen of superbright LEDs.

Figure 1 gives a schematic view of the MPIV system connected to a *personal computer* (PC or laptop). In a typical MPIV session, the PC starts transferring the strobe light pattern to the MPIV memory (RAM). This information is later used by the logic to control the strobe light synchronously with the camera operation. The particles carried by the flow (big left arrow) scatter the strobe light emitted by a *laser pointer* (laser diode). The scattered light is transformed in digital information by a single CMOS camera chip. The logic transfers the picture data from the camera to the MPIV memory where they replace the strobe light pattern. Finally, the computer downloads the images from the MPIV memory and computes the velocity field. Figure 2 shows a

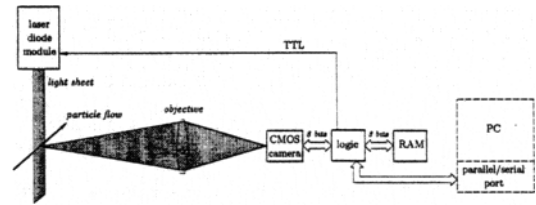


Fig. 1 Schematic view of the MPIV system

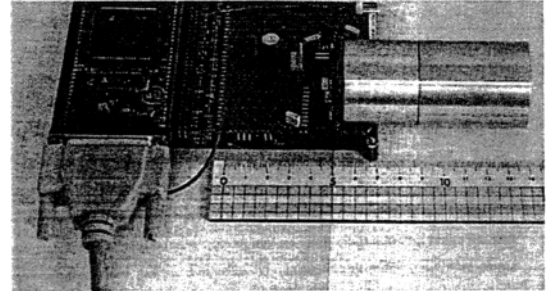


Fig. 2 MPIV prototype

picture of the MPIV prototype.

## 2. Design Outlines

### 2.1 CMOS camera

Our one-chip progressive-scan camera with digital output, produced by OmniVision (1997), is of type CMOS which is somehow different from the well-known CCD cameras. Unlike CCD cameras, CMOS cameras use the same technology as almost all current digital devices. This results in two main advantages. First, CMOS cameras are very cheap. Second, it is very easy to integrate other functionalities on the same chip such as complex logic circuits, ADC, RAM, CPU, etc, which results in a smaller and cheaper system. The best performances are still obtained with the CCD cameras, but the CMOS cameras improve every year. Our CMOS camera is very cheap (less than 50 \$). However, since it was not designed specially for PIV applications, the shutter is of the rolling type (in opposition of synchronous shutter).

With a *synchronous shutter*, it is possible to choose the time of two laser pulses in such a way that one pulse freezes the particle motion in one picture and the second in the next picture. The

picture rate is 20 ms (for 50 Hz cameras), but the time between two pulses may be just a couple of microseconds (the time needed for the CCD camera to transfer the charges from the sensitive image array to the transfer image array). The cross-correlation technique can then be used to determine the flow velocity field. On the other hand, with a *rolling shutter*, getting two independently exposed pictures is possible only when the pulses are at least the picture-scanning time apart. In our system, the scanning time is about 13.8 ms (image  $288 \times 216$ ). For shorter pulse intervals, a part of the picture is exposed twice, and a part is exposed once. This is a *complication* for the image processing — but not a really serious *limitation*. Cross and auto-correlation methods may be combined together. Other approaches may use more than two pulses, since our MPIV system can be programmed with virtually any strobe light pattern (see Sect. 2.4).

Our CMOS camera is connected to a data and address bus, and most of its parameters are configurable through registers. For example, the exposure time (size of the shutter) and the gain can be either in automatic mode, or set to some specific values. The size of the pictures is also configurable. The biggest picture has a resolution of  $384 \times 288$ . In the present prototype, however, the RAM memory (128 K) is too short to store two of these pictures, but two  $288 \times 216$  pictures fit.

## 2.2 Camera objective

The camera objective is made by two doublets resulting in an  $f$ -value of  $f_{\#}=1.4$ , a magnification of  $M=1/2$ , and a particle-to-lens distance of  $s=100$  mm (about 125 mm in water). The observation area is  $6.4 \text{ mm} \times 4.8 \text{ mm}$  (image  $288 \times 216$ ), which is twice bigger than the camera sensitive area (because of the objective magnification  $M$ ).

The objective  $f$ -value is low in order to collect as much light as possible. Classically, small  $f$ -values are limited by lens aberrations (which considerably increase for small  $f$ -values, Jenkins and White, 1981). However, in PIV systems more

lens aberrations may be tolerated, since what really matters is the position of the particles, not their exact portrait. Quantitatively, the size of a particle image (diameter  $d$ ) can be calculated by summing the square of the different contributions (Adrian 1997):

$$d^2 = d_p^2 + d_r^2 + d_i^2 + d_a^2 + d_F^2 + d_s^2 \quad (1)$$

where  $d_p$  is the diameter of the particle image due to the particle size,  $d_r$  is the blur caused by the particle motion (during the exposure period),  $d_i$  and  $d_a$  model the out-of-focus and lens aberration contributions (geometrical optics),  $d_F$  is the Fraunhofer diffraction (wave nature of light) and  $d_s$  the contribution due to the integration of light over a pixel. When all diameters are taken at the “inertia circle,” this formula is exact for any distribution (i. e., not limited to Gaussian). However, the different contributions are assumed independent, which is not rigorously the case (for example, there is some small coupling between lens aberrations, out-of-focus and Fraunhofer diffraction).

For in-focus particles ( $d_i=0$ ), the dominant contribution is usually due to the lens aberrations (at least for low  $f$ -values). However, the modeling of the lens aberration is difficult and very few articles give some explicit expression. Even if the most accurate way remains the geometrical simulation of a bunch of rays going through the lens of the objective (ray tracing), analytical expressions give important information regarding how  $d_a$  varies with respect to the objective main parameters  $M$ ,  $f_{\#}$  and  $s$ . Stanislas and Monnier (1997) mention an analytical results for the spherical aberrations of a plano-convex lens, but a minimal practical objective would contain at least, let's say, two cemented doublets. For such an objective, one can proceed by simulation (ray tracing) and find an appropriate experimental model. Doing so, we extend the model recalled by Stanislas and Monnier (1997) to all aberrations (ray tracing does not “classify” the lens aberrations). For a plano-convex, we obtained (which is, for  $h=0$ , equivalent to the model used by Stanislas and Monnier, 1997)

$$d_a \approx 2s(0.026/f_{\#}^3 + 0.235 h^3/s^3) \quad (2)$$

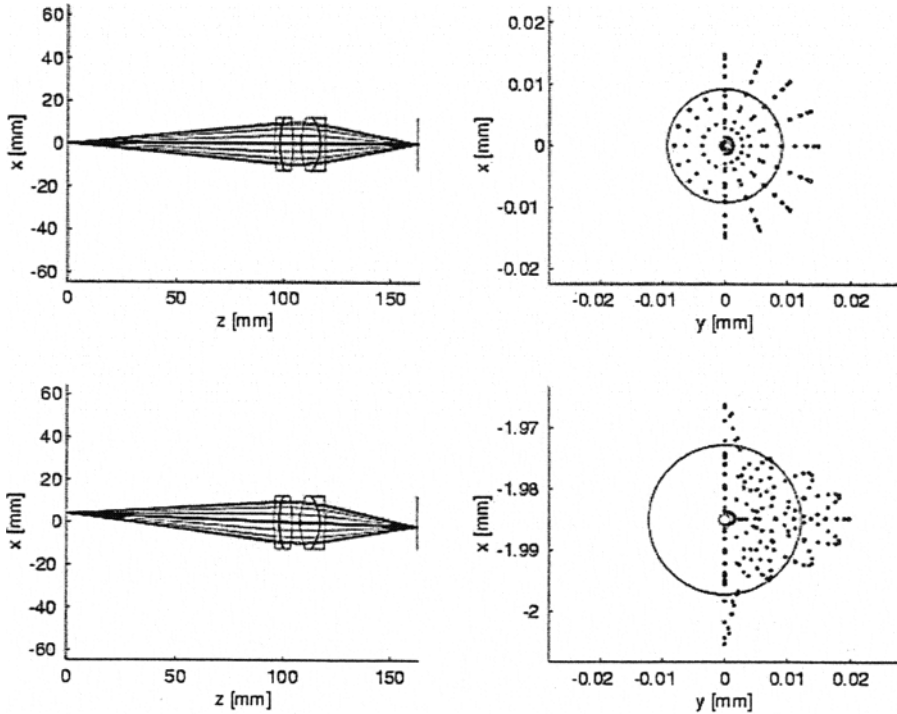


Fig. 3 Ray tracing for a typical MPIV objective ( $s=100\text{mm}$ ,  $M=0.5$ ,  $f_{\#}=1.67$ )

where  $d_a$  is the minimum diameter (measured at the “inertia circle” of the best focused luminous point image), and  $h$  is the distance of the luminous point to the axis (for spherical aberrations,  $h=0$ ). For standard cemented doublets, we obtained the following experimental expression

$$d_a \approx 2s(0.0033/f_{\#}^3 + [0.8559 - 0.0253f_{\#}]^3 h^3/s^3) \quad (3)$$

Note that the spherical aberrations are already reduced by an order of magnitude in comparison to the plano-convex lens (2). Figure 3 shows one simulation done for an objective made of two cemented doublets. Only a few rays are presented for the sake of clarity, but even though the simulations were done with much more rays, the result is very similar to what can be seen in Fig. 3. For these objectives, one can assume that the two lenses are “independent” and estimate the aberrations with the formula

$$d_a^2 \approx M_2^2 d_{a1}^2 + d_{a2}^2 \quad (4)$$

where  $d_{a1}$  stands for the aberrations of the first lens, which are magnified by the second lens of a

factor  $M_2$ , and  $d_{a2}$  is the aberrations of the second lens. With (3), one obtains for  $h=0$  ( $h$  does not vary much in PIV applications, as one can see in Fig. 3 where one particle on the optical axis and one at the corner of the observation area are simulated):

$$d_a \approx 0.0066 Ms(M^6 + 1)^{1/2} / f_{\#}^3 (1 + M)^3 \quad (5)$$

where  $M$ ,  $s$  and  $f_{\#}$  are the objective parameters (magnification, distance to the in-focus plane and  $f$ -value).

Figure 4 shows the results obtained for many simulations of different objectives compared with the above formula. Both simulation results and model are normalized with respect to  $M$  and  $s$ , i. e.,  $d_a^{norm} = d_a(1 + M)^3 / Ms(M^6 + 1)^{1/2}$ .

The lower the  $f$ -value, the more light is collected by the objective but also the bigger is the particle image. To obtain the best of the available camera resolution, oversampling of particle images should be avoided (Adrian, 1997). In our camera, the pixel size is  $11\mu\text{m}$ , which is compatible with the proposed objective of Fig. 3.

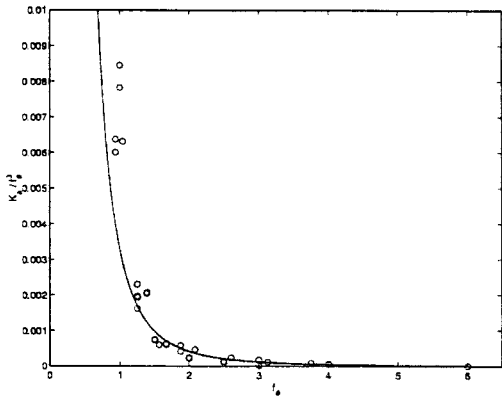


Fig. 4 Spherical aberrations, simulation (circle) and model (solid line)

### 2.3 Laser diode module

Transverse illumination is achieved by a cheap (\$ 50) laser diode module similar to a pointer laser. The dimension of the module is about dia. 10 mm×25 mm. The light is red (650 nm) and the emitted power does not exceed 5 mW. The module includes a collimating optics that produces a beam about 4 mm wide and 1 mm thick. Such a beam can be readily used without the need of any additional optics. This cheap module is designed for continuous wave (CW) operation, but a modulation up to 10 kHz was experimentally shown possible.

As far as chromatic lens aberrations are con-

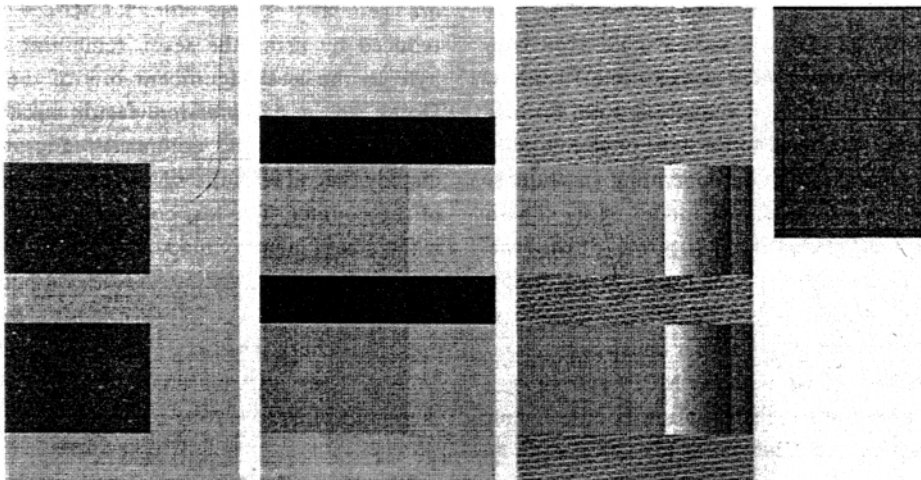


Fig. 5 Time diagram, strobe pattern diagram, compression diagram and memory map (image 288×216)

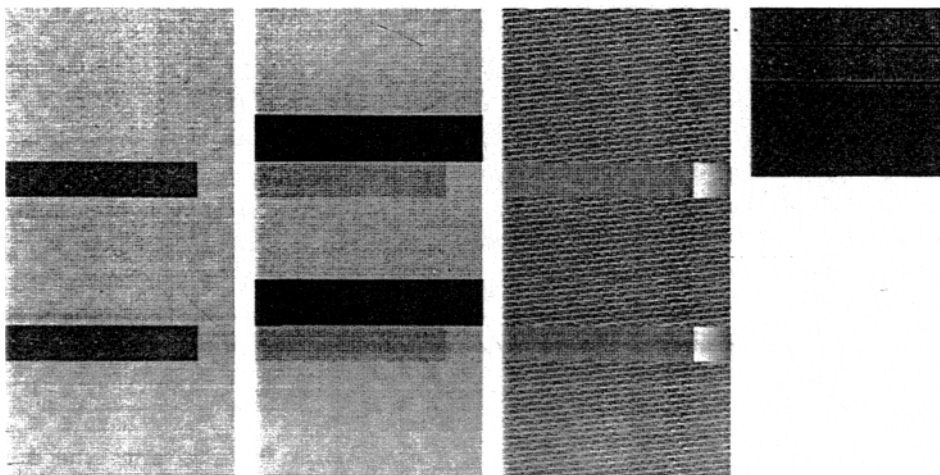


Fig. 6 Time diagram, strobe pattern diagram, compression diagram and memory map (image 384×72)

cerned, laser diodes emit monochromatic light. Therefore, achromatic lenses are not required and cheaper lenses can be used. Lens coating, however, is recommended, since it limits reflection and light lost to the minimum. Visible red or infrared light is a good choice for MPIV systems since the camera and the laser diodes have their best efficiency for this light color.

Experimental tests (see Sec. 3) have shown that the minimum beam illuminance needed to visualize white glass particles (dia 10  $\mu\text{m}$ ) in water is about 25  $\mu\text{J}/\text{mm}^2$ . As the exposure time of a 50 Hz camera is limited to 20 ms, the maximum illuminance emitted by the laser pointer is about 25  $\mu\text{J}/\text{mm}^2$ . The laser pointer is therefore just powerful enough to visualize particles. However, the maximum velocity at 20 ms is around 10 mm/s. A more useful maximum velocity around 50 m/s would need 5000 times more light power. Nowadays, compact laser diodes operating in a quasi continuous wave (QCW) mode exist. These diodes can easily emit such a power during the needed 4  $\mu\text{s}$ . Even though the price of these high-power laser diodes is getting lower and lower, they are still expensive. Another cheap alternative to measure faster flow with the MPIV system uses LEDs in a backward illumination configuration and is described in Chetelat et al. (2001).

#### 2.4 Strobe light pattern

In order to generate a given strobe light pattern, first the PC has to program the MPIV system. Then, the PC sends a special "start" signal to the MPIV system. In response to this signal, the MPIV system waits for the camera beginning the scanning of a new picture, and then starts generating the strobe light pattern.

As a picture may be (at least partially) exposed during the time covering the scanning of the previous and the actual frames, the strobe pattern is defined during three frames (even though only the two last pictures are captured). The first column of Figs. 5 and 6 shows the position of the two captured pictures with respect to the three frames in which the strobe light is programmed.

The time resolution of our MPIV system is 140

ns. This excellent resolution is achieved by using the camera pixel clock to increment a counter that points at subsequent RAM locations in which a bit indicates if the laser diode state (ON/OFF) has to be toggled (bit is 1) or maintained (bit is 0). The programming of any pattern is virtually possible and straightforward: the whole RAM is set to 0, except for the locations corresponding to ON/OFF transitions (which are set to 1). The second column of Figs. 5 and 6 show (in black) the time during which the light has to be ON. The programming of such a pattern is a 1 at every (here four) transition, and anywhere else 0.

As the transitions ON/OFF defining the pulses are generally sparse, the RAM size may be reduced by using the seven remaining bits of a byte as the least significant bits of the counter. Doing so, a compression factor up to 128 is obtained. The third column of Figs. 5 and 6 display the value of the seven least significant bits of the counter. The last column of Figs. 5 and 6 is the actual memory map. The black zone is only what is needed to encode the strobe pattern outside the pictures. The gray zone after the second picture is the unused memory. This memory can be used to program more ON/OFF transitions for more complicated strobe light patterns.

#### 2.5 Image buffer

The pixels getting continuously out the camera by burst at more than 7 MHz have to be stored in a buffer since the transfer rate to the PC is an order of magnitude slower. The task performed by the logic circuit is fairly simple:

1. read current byte from RAM memory;
2. if 0, maintain light state, toggle otherwise;
3. read current pixel value from camera;
4. store it in current RAM location (as a replacement of the strobe data now used);
5. increment counter (current RAM address).

The logic used to implement this algorithm is a cheap programmable CPLD (XC95108 from Xilinx, 1998).

Since during the first frame and during the horizontal and vertical synchronization period of

the two other frames the camera does not output any pixel, nothing have to be stored and the compression scheme addressed in Sec. 2.4 is used to considerably reduce the amount of memory needed. Our 128K-byte memory is large enough to store two consecutive images ( $288 \times 216$ ) exposed by virtually any strobe light pattern.

Our MPIV system uses another refinement to speed up the transfer of the pictures and the programming of the strobe light pattern. As almost all RAM locations have to be reset to 0 for the strobe light pattern, right after the reading of a picture byte by the PC, the MPIV logic automatically resets the corresponding location to 0. In addition, the logic increments the RAM counter to spare the PC the need to transfer a new RAM address.

### 2.6 Communication with PC

The communication with the personal computer is performed via the parallel port (ECP

protocol, Voth et al., 1993), which is standard on PCs and allows transfer rates up to 2 Mbytes/s (other protocols, like USB [universal serial bus], could equivalently be implemented). Extra hardware such a frame grabber acquisition board is not required. The MPIV system readily works with any PC or laptop on which only a small driver application (software) has been installed.

## 3. Experimental Results

Figures 7 and 8 show the results obtained for (twice) three experiments (one row is one experiment). In the first column is the first picture. The next picture taken 20 ms later is in the second column. In the third column is the velocity field computed with a classical approach using cross-correlation technique (since the pulses are here far enough apart).

In the two first experiments, the laser is in continuous wave mode. As the CMOS camera has

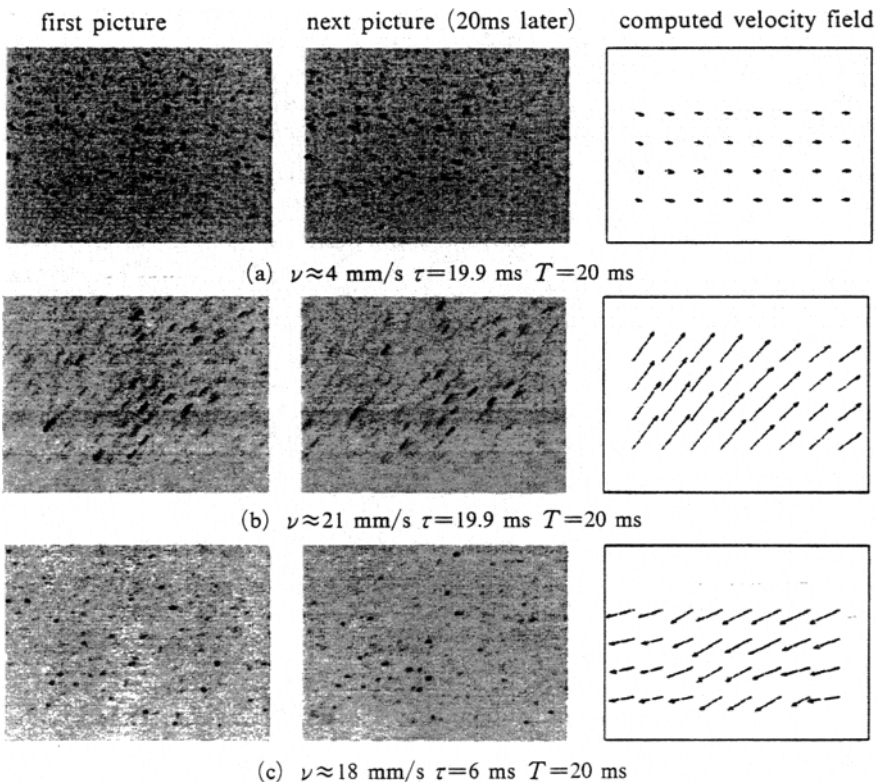


Fig. 7 Experimental results (image  $288 \times 216$ )

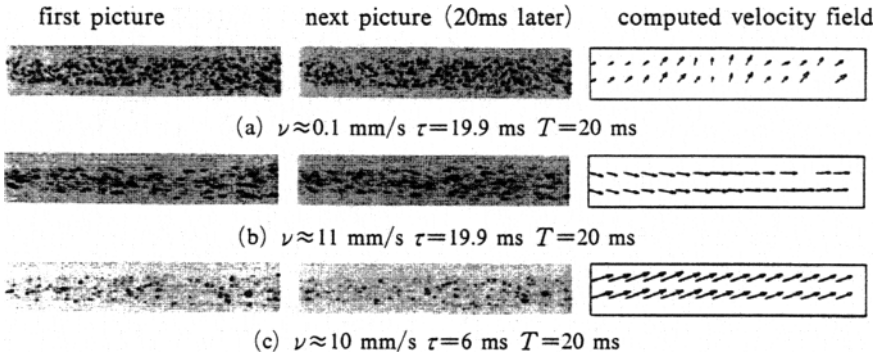


Fig. 8 Experimental results (image  $384 \times 72$ )

a rolling shutter, one row is always busy transferring its data. During this time, the row is not sensitive to the light. As 20 ms corresponds to 312.5 rows, the effective exposure time is  $\tau = (312.5 - 1) / 312.5 \times 20 \text{ ms} = 19.9 \text{ ms}$ . The time between two expositions is  $T = 20 \text{ ms}$ .

The last experiment uses the laser in pulsed mode. The time separating two pulses is  $T = 20 \text{ ms}$ , and the pulse duration is set to  $\tau = (312.5 - 216) / 312.5 \times 20 \text{ ms} = 6 \text{ ms}$  (where 216 is the number of picture rows) to expose only one picture per pulse (see illustration at Fig. 5, respectively Fig. 6). A longer time would partially expose also the following picture.

#### 4. Conclusion

This paper demonstrates that PIV-based sensors may be small, easy-to-use and cheap thanks to the recent development of electronics. Original design ideas include the use of a laser diode for illumination and a CMOS camera for imaging. Our MPIV system constitutes a first prototype (which is fully operational but limited to slow flows). Significantly better performances should be achieved with a QCW laser diode (which can be, for short pulses, more than 5000 times more powerful than a laser pointer). To keep the price low, another alternative may use a different illumination strategy. For example, superbright LEDs in a backward illumination configuration turned to give (much) better results. A larger memory would also enable to

store bigger (or more) pictures for a negligible cost increase.

#### Acknowledgment

This work has been supported by a grant from Brain Korea 21 project.

#### References

- Adrian R. J., 1997, "Dynamic Ranges of Velocity and Spatial Resolution of Particle Image Velocimetry," *Measurement Science and Technology*, volume 8, pp. 1393~1398.
- Chetelat O., Yoon, S. Y. and Kim, K. C., 2001, "Miniature PIV System (MPIV) With LED in-Line Illumination," *Proc. of 4<sup>th</sup> International Symposium on Particle Image Velocimetry (PIV01)*, Goettingen, Germany, paper 1059.
- Degrez G., Riethmuller M. L., 1994, "Optical Measurements," *Measurements Techniques in Fluid Dynamics, An Introduction*, Chapter 6, von Karman Institute for Fluid Dynamics, pp. 229~300.
- Jenkins F. A. and White H. E., 1981, *Fundamentals of Optics*, Mc Graw-Hill, Singapore.
- Lourenco L. M., 1996, "Particle Image Velocimetry," *Lecture series 1996-03*, von Karman institute for fluid dynamics, 1~110.
- OmniVision, 1997, "OmniVision OV5017," <http://www.ovt.com/pdfs/OV5017DS.pdf>.
- Stanislas M. and Monnier J. C., 1997, "Practical Aspects of Image Recording in Particle

Image Velocimetry,” *Measurement Science and Technology*, Vol. 8, pp. 1417~1426.

Voth D., Taylor R., Williams F., Styles R. and Mouhanna J., 1993, “Extended Capabilities Port: Specifications,” <http://www.fapo.com/files/ecp>

*-reg.pdf*, Rev. 1.06.

Xilinx, 1998, “XC95108 In-System Programmable CPLD,” <http://www.coolpld.com/index.shtml>.